

I. Dominguez, I. del Villar, J. Corres, J. Lachaud, Y. Yang, H. Hallil, C. Dejous and I. R. Matias, *Analyst*, 2022, **147**, 5477

**DOI:** 10.1039/D2AN01371A

## Electronic Supplementary Information

# Spectral measurements with hybrid LMR and SAW platform for dual parameter sensing

Ismel Dominguez<sup>1</sup>, Ignacio del Villar<sup>1,2</sup>, Jesús Corres<sup>1,2</sup>, Jean-Luc Lachaud<sup>3</sup>, Yang Yang<sup>3</sup>, Hamida Hallil<sup>3</sup>, Corinne Dejous<sup>3</sup>, Ignacio R. Matias<sup>1,2</sup>

<sup>1</sup> Electrical, Electronic and Communications Engineering Department, Public University of Navarra, 31006 Pamplona, Spain.

<sup>2</sup> Institute of Smart Cities (ISC), Public University of Navarra, 31006 Pamplona, Spain.

<sup>3</sup> Univ. Bordeaux, CNRS, Bordeaux INP, IMS, UMR 5218, F33400, Talence, France.

### 1. Detailed aligner and test cell setup

To correctly guide the light through the SiO<sub>2</sub> substrate of the SAW sensor, the help of an aligner is needed. To improve the alignment, the design included a stepper motor control with microstepping technology, so that the alignment of the optical fibers with the substrate is much more precise. The commonly used SAW sensor test cell was modified to give access to the optical fibers. All parts are made of PMMA and are attached to the electronic board with the help of screws. The designed and built setup and modified test cell parts are shown in detail in **Figure S1**.

The LW-SAW test cell was modified starting from a previous design, allowing the alignment of two 230 μm MMF fibers to the fine silica surface layer of the acoustic transducer of about 5 μm. The adaptation consists of removing part of the cell that holds the LW-SAW sensor so that the mechanism that holds the multimode optical fibers can access the SiO<sub>2</sub> guided layer of the acoustic sensor.

Taking into account that the LW-SAW sensor has a 5  $\mu\text{m}$  thick  $\text{SiO}_2$  layer, the help of an aligner is essential to accommodate the greatest amount of light and have a better visualization of the resonance. It also helps in the fixation and immobilization of the sample while the different liquids are introduced. Any movement of the sample can introduce reading errors in the acoustic and optical parts.

A double-glue coated film from X-film, Montex DX 2, was used to join the bottom part of the microfluidic test unit and the SAW-LMR sensor. The thickness of this film is 70  $\mu\text{m}$  and it is made of transparent monomeric PVC, which offers great resistance to chemical agents. It has a coating in the form of permanent glue that offers an adhesive force of  $\geq 22 \text{ N} / 25 \text{ mm}$ , guaranteeing a great seal despite the small contact area between the sensor and the part that supports the tubes. This joint gasket has been cut on a Silhouette Cameo 3 model xurography device. The volume of the sensor chamber is around 10  $\mu\text{L}$ .

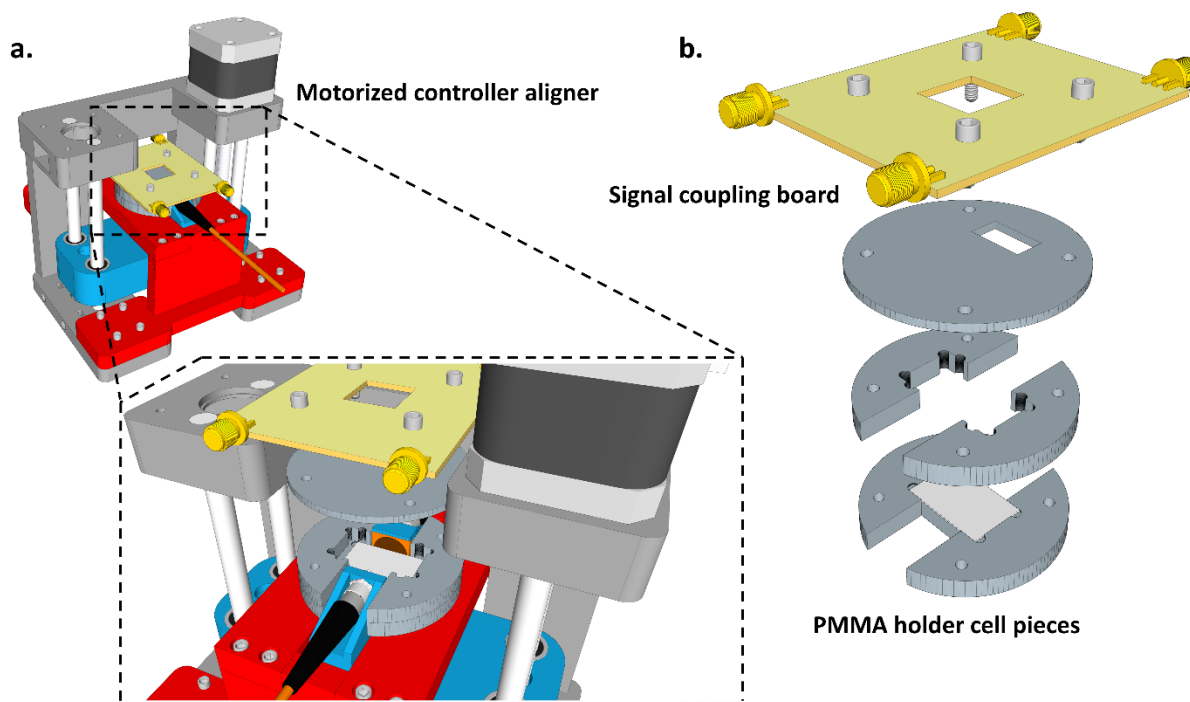


**Figure S1.** (A) Detail of the motorized aligner. (B) PMMA parts of the adapted test cell and contact electronic board.

## 2. SAW calibration

The operating principle of the SAW sensor shows an attenuation of the signals transmitted and reflected in the waveguide when its surface comes into contact with a liquid. The attenuation experienced by the sensor due to the transition from air to water is shown in **Figure S2**. The S21 parameter decreases almost -10 dB at the central frequency (around 118 MHz).

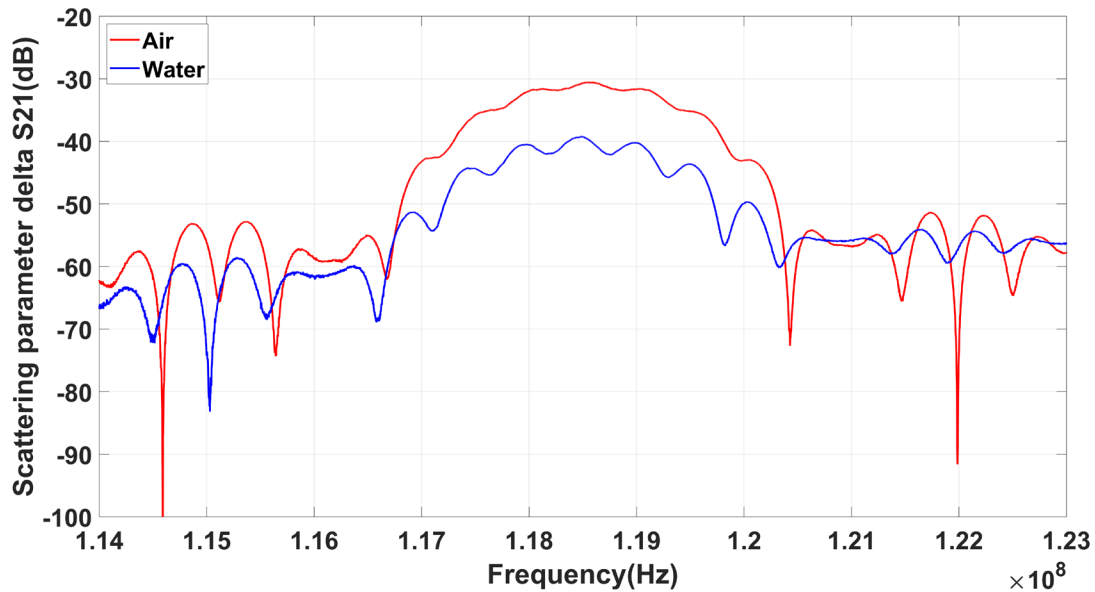


**Figure S2.** Transmission attenuation (S21 parameter) of the delay line exposed to air and exposed to water.

### 3. Hybrid sensor, LMR and SAW sensorgram analysis

The responses of both sensors, SAW-S11 and LMR1, are represented in **Figure S3**. It can be seen that both responses are synchronous with respect to each other.

With a less precise response from the LMR2 resonance, in the same way and synchronously, the evolution of both sensors can be observed. The  $\Delta S_{21}$  and  $\Delta S_{11}$  parameters are compared to LMR2 response respectively in **Figure S4** and **Figure S5**.

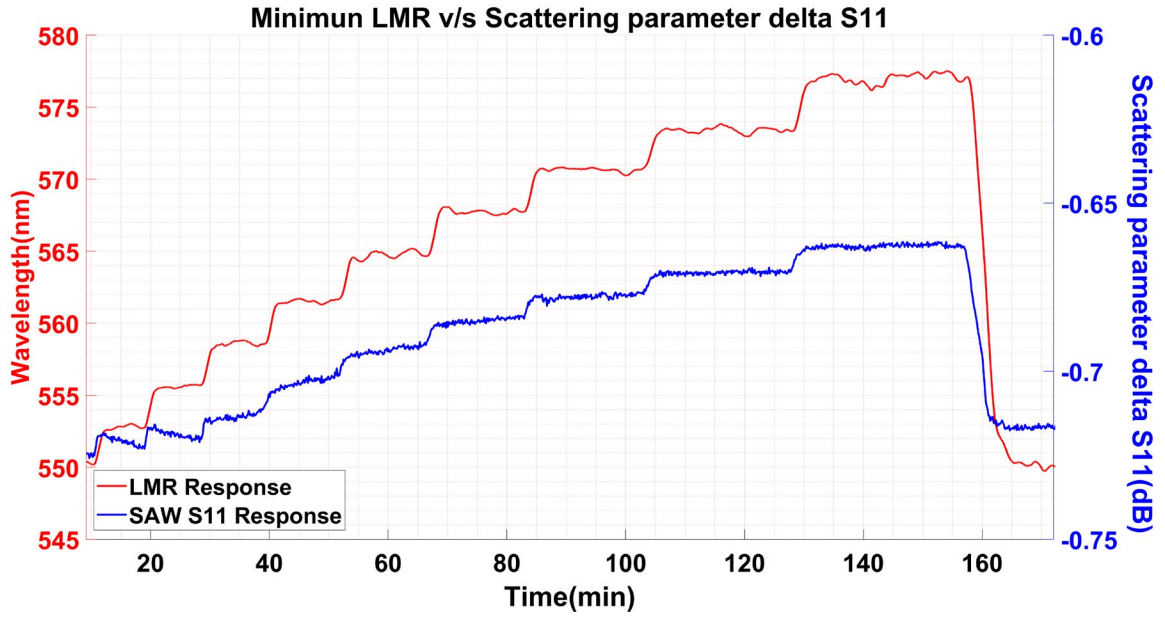


Figure S3. Sensorgram of LMR1 and S11 parameter shift of SAW.

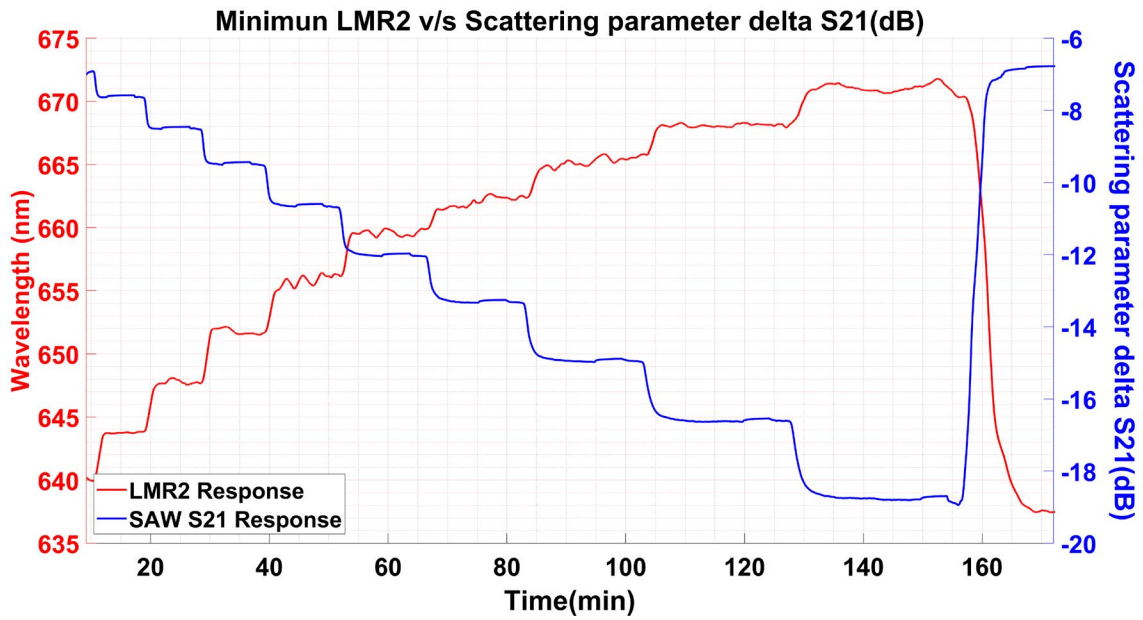


Figure S4. Sensorgram of LMR2 and S21 parameter shift of SAW.

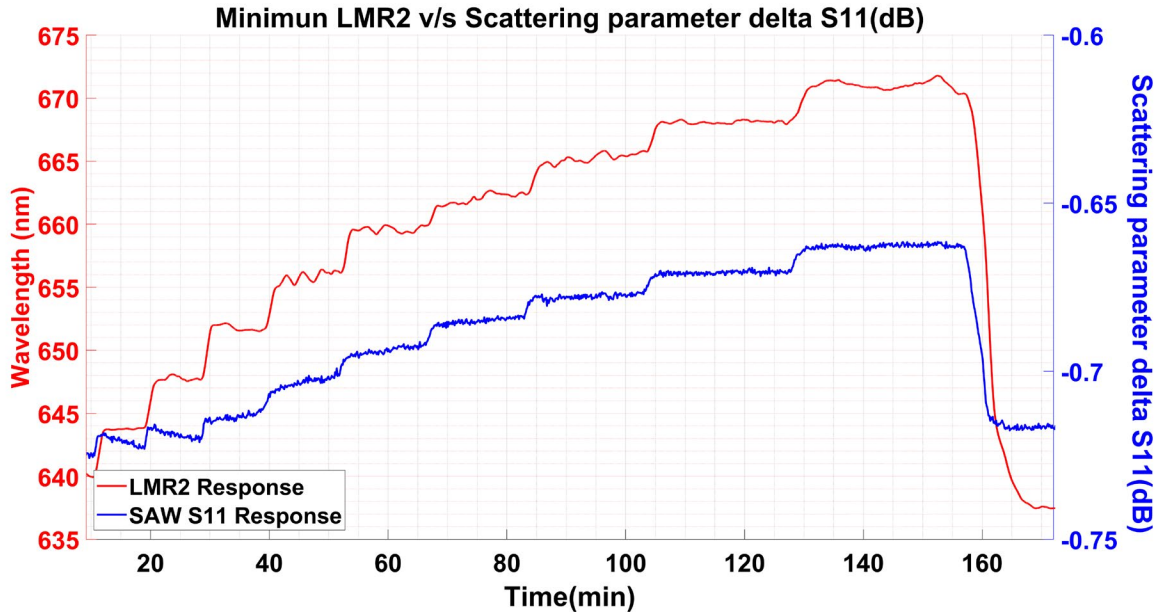


Figure S5. Sensorgram of LMR2 and S11 parameter shift of SAW.

#### 4. LMR1 calibration

It is known that depending on the thickness of the thin film it is possible to observe more than one LMR resonance simultaneously. In the deposition carried out, two first-order resonances were obtained, in transverse magnetic mode, at wavelengths of 550 nm and 640 nm, which have been named LMR1 and LMR2, respectively. Thanks to the continuous monitoring of the experiment carried out in **Figure S6**, it is possible to observe the evolution of both resonances.

To analyze the evolution of the minimum of the LMR1 and LMR2, a second order polynomial approximation was applied. The evolution of the LMR1 resonance can be seen in **Figure S7**. In the same way, the evolution of the LMR2 is observed in **Figure S8** with a saturation of the signal for higher refractive indices.

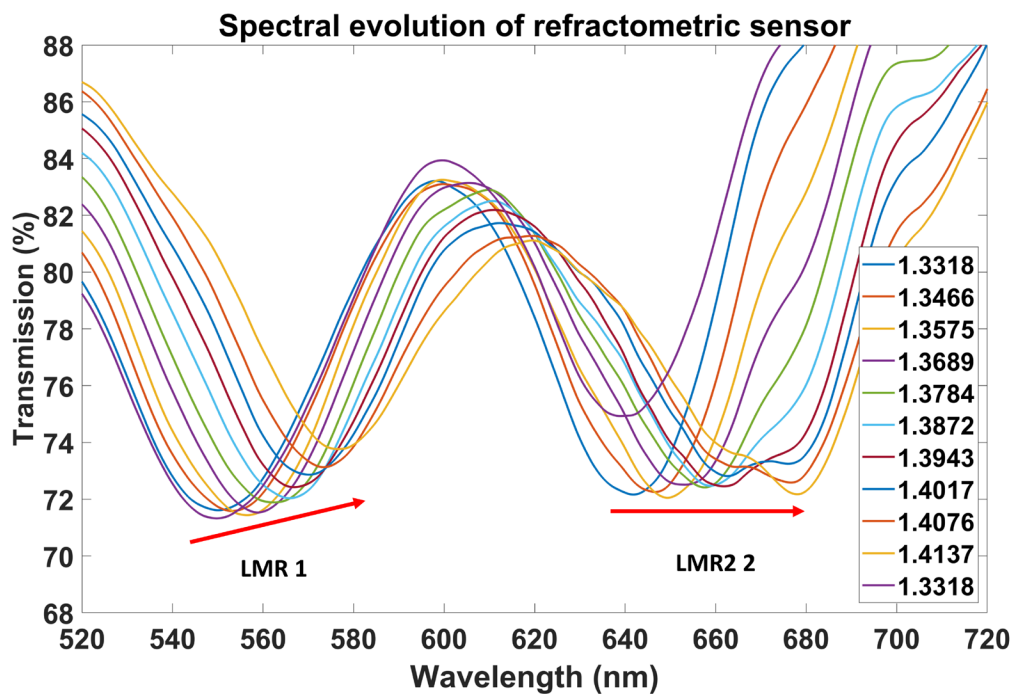


Figure S6. Wideband spectra including LMR1 and LMR2 at each steady-state of the experiment.

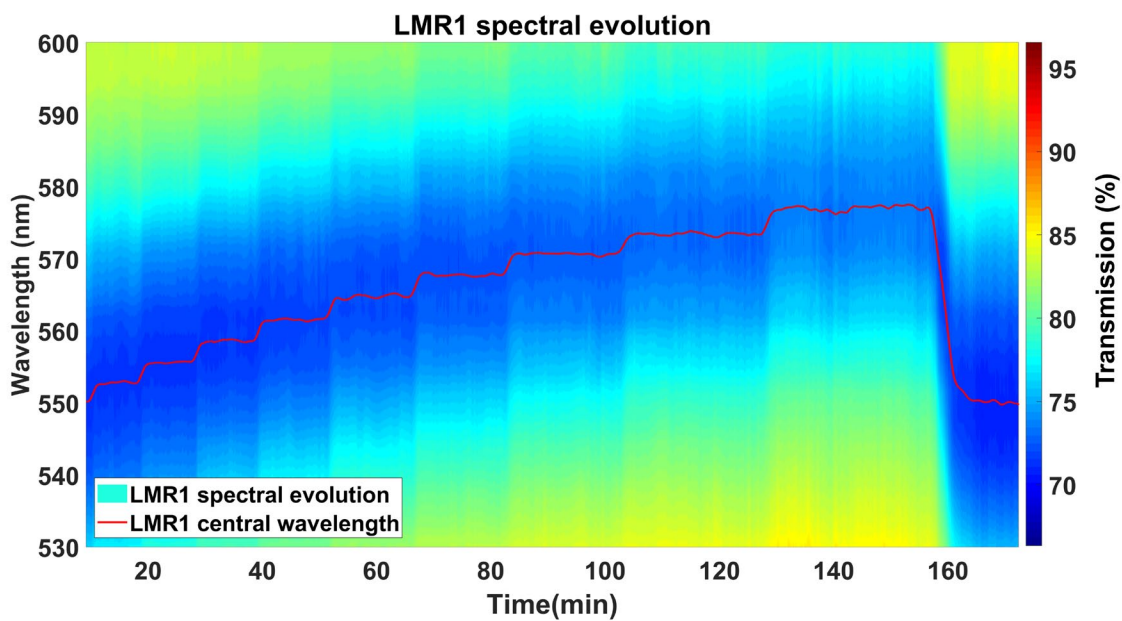


Figure S7. Spectral evolution of the LMR1.

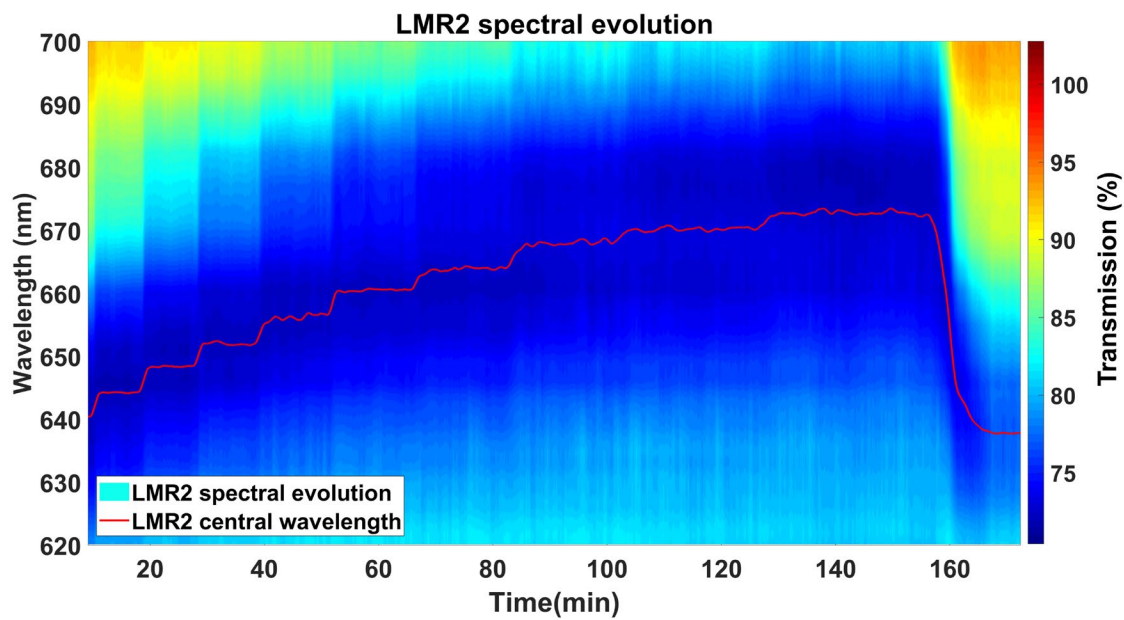


Figure S8. Spectral evolution of the LMR2.